JOURNAL OF CATALYSIS 154, 306–313 (1995)

Novel Support Effects on the Mechanism of Propene–Deuterium Addition and Exchange Reactions over Dispersed ZrO_2

Shuichi Naito*,[1] and Mitsutoshi Tanimoto†

*Department of Applied Chemistry, Faculty of Engineering, Kanagawa University, 3-27-1, Rokkakubashi, Kanagawa-ku, Yokohama 221, Japan; and †Department of Chemistry, Faculty of Science, Shizuoka University, 836 Ohya, Shizuoka 422, Japan

Received June 27, 1994; revised December 19, 1994

The effect on the rate and mechanisms of propene–deuterium reactions of dispersing ZrO_2 on various supports such as silica, alumina, and titanium dioxide has been studied by microwave spectroscopic analysis of monodeuteropropene as well as by kinetic investigation. By dispersal of ZrO_2 on these supports, the rate of the C_3H_6–D_2 reactions is increased considerbly compared to that over unsupported ZrO_2, with the decrease of activation energy. Hydrogen exchange in propene proceeds simultaneously with addition via the associative mechanism through *n*-propyl and *s*-propyl intermediates. Through XPS analysis of ZrO_2/SiO_2, it was found that a monolayer of ZrO_2 is formed over the silica support. The monolayer catalyst exhibits catalytic behavior quite different from that of unsupported ZrO_2. On the other hand, alumina surfaces modified by ZrO_2 layers may be the main active sites in the case of ZrO_2/Al_2O_3. The marked enhancement of the reaction rate in the lower loading region of ZrO_2/TiO_2 may be explained by the strong interaction of atomically dispersed zirconium ions with active centers on TiO_2.

INTRODUCTION

The nature of a support material as well as the particle size of a metal greatly influences the activity and the selectivity of the catalytic reaction over supported metal catalysts (1). The morphological change of the metal with particle size and its electronic interaction with the support may be the main factors that control the reactions (2, 3).

It has been demonstrated that two-dimensional metal oxide overlayers are formed when one metal oxide, such as Re_2O_7 (4), Cr_2O_3 (5), V_2O_5 (6), Nb_2O_5 (7), MoO_3 (8), or WO_3 (9), is dispersed on a second metal oxide with high surface area as support (SiO_2, Al_2O_3, or TiO_2). The surface structure of these overlayers has been investigated extensively with various spectroscopic techniques (10), and the correlations between the structure and the catalytic behavior of the supported metal oxides have been examined in some catalytic reactions (11, 12).

Recently, we have studied C_3H_6–D_2 and C_3H_6–C_3D_6 reactions over unsupported and supported ZrO_2 catalysts on various oxides and briefly reported that the catalytic behavior of zirconium oxide changed remarkably when it was supported on silica, alumina, or TiO_2 (13). In the present study, we applied an isotopic tracer technique to elucidate the mechanistic difference over these catalysts. Microwave spectroscopy is a powerful technique for the study of hydrogen exchange processes because it enables us to determine the hyperfine distribution of the D atom in the exchanged propene-d_1 molecule, which directly reflects the previous points of attachment of the adsorbed molecules onto the catalysts (14). In the C_3H_6–D_2 reaction, the reactivity ratio of *n*-propyl to *s*-propyl intermediates is estimated from these isotopic distributions. Accordingly, this technique enables us to monitor the dependence of not only the reaction rates but also the reaction intermediates on the particle sizes of the supported oxides and the nature of the supports.

EXPERIMENTAL

Catalyst Preparation

Support powders (SiO_2, Aerosil 300; Al_2O_3, aluminum oxide-C; and TiO_2, P-25 from Nippon Aerosil), evacuated at 723 K for 2 h, were injected into appropriate dried hexane solutions of $Zr(OC_3H_7)_4$ (Soegawa Chemicals) under a nitrogen atmosphere and were stirred vigorously overnight. After removing the solvent by vacuum distillation, the catalyst was oxidized overnight with O_2 at 923 K. The unsupported ZrO_2 catalyst was prepared by adding a small amount of water to the hexane solution of $Zr(OC_3H_7)_4$, followed by filtration, drying, and oxidation. Commercial ZrO_2 powder (Soegawa Chemicals) was also employed as an unsupported catalyst. The XPS (X-ray photoelectron spectrum) was measured with ESCALAB-

[1] To whom correspondence should be addressed.

0021-9517/95 $12.00

5, using Mg$K\alpha$ as an X-ray source. To calibrate binding energies, Au 4*f* 7/2 (83.7 eV) was used as a reference.

Reaction Procedure and Detection Methods

Gaseous H_2 and D_2 from a commercial cylinder were purified by circulating them over a heated Pd black catalyst to remove trace amounts of oxygen. C_3H_6 (Takachiho Kagaku K.K.), C_3D_6, and $H_2C{=}CD{-}CH_3$ (Merck, Sharp and Dohme Ltd.) were purified by a freeze–thaw cycle. $HDC{=}CH{-}CH_3$ was prepared from 1-bromoprop-1-ene according to the procedure described in the literature (15).

The catalyst (ca. 1 g) was put in a quartz reaction cell which was connected to a closed gas circulation system (total volume: ca. 300 cm^3). Before each run the catalyst was freshly oxidized by O_2 at 623 K for 2 h, followed by evacuation at the same temperature for 30 min. After cooling to the reaction temperature, a mixture of the reaction gases was admitted into the system. At certain intervals during the reaction, a small percentage of the circulating gas was sampled and separated into propane and propene by gas chromatography (alumina column, He carrier). The deuterium contents in the formed propane and the exchanged propene were determined with a mass spectrometer (Hitachi RMU-6MG) at 15 and 12 eV ionization voltage, respectively. The location of the deuterium atom in monodeuteropropene was determined by recording the microwave absorption line (1_{01}–0_{00} rotational transition) characteristic of each isotopic species. The isotopic isomers in monodeuteropropene were denoted as follows:

c-1-d_1 :

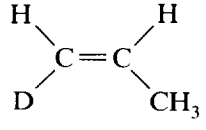

2-d_1 : $H_2C{=}CD{-}CH_3$

t-1-d_1 :

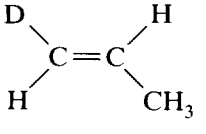

3-d_1 : $H_2C{=}CH{-}CH_2D$.

RESULTS

1. Characterization of Supported Catalysts

Figure 1 shows the XPS spectra of various catalysts investigated in this study. On dispersal Zr3$d_{5/2}$ peaks shifted 0.5–1.0 eV toward the higher binding energy side, suggesting a certain electronic interaction of dispersed ZrO_2 with the supports. It is well known that XPS intensity ratios reflect aspects of the surface structure of the catalysts, such as the extent of dispersion of supported metal or oxides (16–18). When a supported oxide surface is covered by a uniform zirconia layer of thickness d and coverage θ, the intensity ratio I_{Zr}/I_{Sup} of the Zr3d peak to the 2s and 2p peaks of the support atoms (Si2s, Al2p, or Ti2p) at the electron takeoff angle 90° from the surface plane can be expressed as (16)

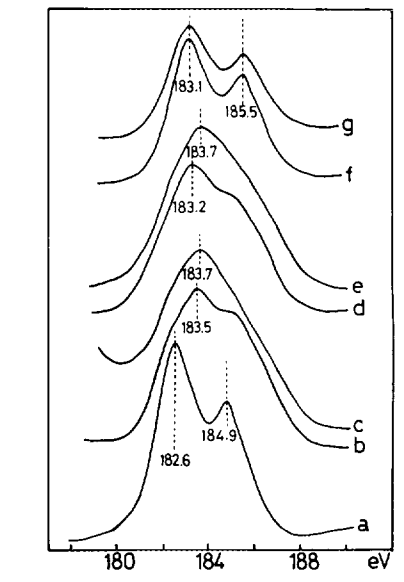

FIG. 1. Zr3$d_{3/2}$ and Zr3$d_{5/2}$ XPS spectra of unsupported and supported ZrO_2 catalysts: (a) unsupported ZrO_2, (b) 8 wt% ZrO_2/SiO_2, (c) 1 wt% ZrO_2/SiO_2, (d) 10 wt% ZrO_2/Al_2O_3, (e) 1 wt% ZrO_2/Al_2O_3, (f) 10 wt% ZrO_2/TiO_2, and (g) 1 wt% ZrO_2/TiO_2.

$$\frac{I_{Zr}}{I_{Sup}} = \frac{I^0_{Zr}}{I^0_{Sup}} \frac{\theta[1-\exp(-d/\lambda_{Zr})]}{1-\theta[1-\exp(-d/\lambda_{Sup})]}, \qquad [1]$$

where the superscript 0 denotes the intensity for an infinitely thick sample and λ_{Zr} and λ_{Sup} are the escape depths of the photoelectrons corresponding to the Zr3d and support levels, respectively. When $1 \gg d/\lambda$ (monolayer of ZrO_2), Eq. [1] can be reduced to

$$\frac{I_{Zr}}{I_{Sup}} = \frac{I^0_{Zr}}{I^0_{Sup}} \frac{d}{\lambda_{Zr}} \cdot \theta. \qquad [2]$$

Table 1 summarizes the coverages θ of ZrO_2 over various supports, estimated from Eq. [2]. The following values were used for the ratios I^0_{Zr}/I^0_{Sup}: ZrO_2/silica = 8.54, ZrO_2/alumina = 10.8, and ZrO_2/titania = 1.34 (19). For d/λ_{Zr} the value 0.2 was used. For 1 wt% catalysts, the coverages (θ_{XPS}) obtained agree reasonably well with the values (θ_{calc}) calculated under the assumption that a two-dimensional network (the surface area of one ZrO_2 unit of the network is assumed to be 20 $Å^2$) is formed over

TABLE 1

Characterization of Supported ZrO_2 by XPS

Catalysts	Loading amount (wt%)	$Zr3d_{5/2}$ B.E. (eV)	I_{Zr}/I_{Sup}	$\frac{(I_{Zr}/I_{Sup})}{(I^0_{Zr}/I^0_{Sup})}$	θ_{XPS}	θ_{calc}
ZrO_2		182.6				
	1.0	183.7	0.075	0.0088	0.04	0.03
ZrO_2/SiO_2	8.0	183.5	0.546	0.064	0.32	0.26
	1.0	183.7	0.116	0.011	0.05	0.10
ZrO_2/Al_2O_3	10.0	183.2	0.432	0.040	0.20	0.99
	1.0	183.1	0.033	0.026	0.13	0.20
ZrO_2/TiO_2	10.0	183.1	0.167	0.13	0.65	1.98

various supports (surface areas: SiO_2, 300 $m^2\ g^{-1}$; Al_2O_3, 100 $m^2\ g^{-1}$; and TiO_2, 50 $m^2\ g^{-1}$). The coverage θ_{XPS} of 8 wt% ZrO_2/SiO_2 is also in good accordance with θ_{calc}, suggesting that zirconia is well dispersed over the silica surface, probably forming monolayers. On the other hand, in 10 wt% ZrO_2/Al_2O_3 and ZrO_2/TiO_2, θ_{XPS} is considerably smaller than θ_{calc}. This result indicates that in higher loading regions zirconium oxide forms multilayers over alumina and titanium dioxide supports.

2. *C_3H_6–D_2 and C_3H_6–C_3D_6 Reactions over Unsupported and Silica-Supported Catalysts*

When a mixture of C_3H_6 (25 Torr : 1 Torr = 133.3 N m^{-2}) and D_2 (100 Torr) was introduced onto unsupported ZrO_2 catalyst, only propane was formed with the corresponding decrease of C_3H_6, which was consistent with the result reported in the literature (20) and was common over unsupported oxide catalysts (21–25). Thus no hydrogen exchange of propene took place on this catalyst and most of the formed propane was $C_3H_6D_2$. The situation was completely different when ZrO_2 was dispersed on SiO_2. Both deuterium addition and exchange of propene proceeded simultaneously on the dispersed catalysts.

The temperature dependence of these processes is summarized in Fig. 2, where the reaction rates are normalized with respect to the unit weight of ZrO_2 instead of the total catalyst weight including the support. The initial rate of propene-d_1 formation over 8 wt% ZrO_2/SiO_2 was twice as fast as that of propane formation in the temperature range investigated. However, the activation energies are the same (E_a = 39–40 kJ/mol) for both the exchange and the addition processes. This result strongly suggests that both processes proceed through the same σ-alkyl reaction intermediates, *n*-propyl and *s*-propyl adsorbed species (associative mechanism as shown in Scheme 1). The initial rates of propane formation over 1 wt% ZrO_2/SiO_2, also

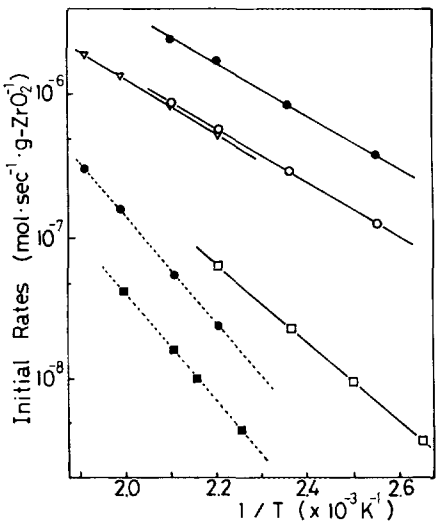

FIG. 2. Temperature dependence of C_3H_6–D_2 reactions (solid lines; P_{C3H6} = Torr, P_{D2} = 100 Torr) and C_3H_6–C_3D_6 reactions (broken lines; $P_{C3H6} = P_{C3D6}$ = 12.5 Torr) over unsupported and silica-supported ZrO_2 catalysts (1 g of catalyst). Open and closed symbols refer to the initial rates of propane and propene-d_1 formation, respectively. ○●, 8 wt% ZrO_2/SiO_2; ▽, 1 wt% ZrO_2/SiO_2; □■, unsupported ZrO_2.

plotted in Fig. 2, yielded the same reaction rates and activation energy as those over 8 wt% catalyst. On the other hand, the initial rate of propane formation over unsupported ZrO_2 was considerably slower than that over supported ZrO_2 and the activation energy was significantly higher (E_a = 53 kJ/mol), as seen in the figure.

Figure 3 demonstrates the time courses of the overall composition of monodeuteropropenes formed during the C_3H_6–D_2 reaction over 1 and 8 wt% ZrO_2/SiO_2 catalysts. At the very beginning of the reaction, the main products were propene-2-d_1 and propene-1-d_1, with a small amount of propene-3-d_1. As the reaction proceeded, a considerable change in the isotopic distribution was observed. If

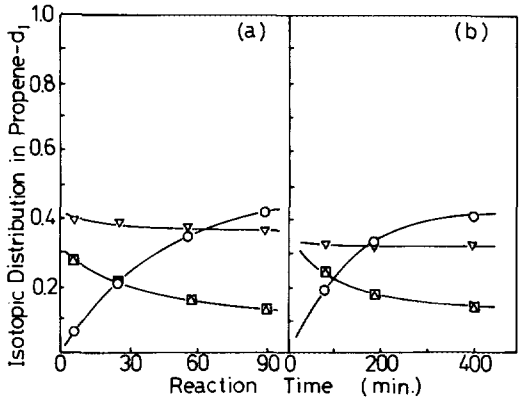

FIG. 3. Time courses of the isotopic distribution in propene-d_1 formed during C_3H_6–D_2 reactions at 423 K (a) aover 8 wt% ZrO_2/SiO_2 and (b) over 1 wt% ZrO_2/SiO_2. P_{C3H6} = 25 Torr, P_{D2} = 100 Torr. One gram of catalyst. □, c-1-d_1; △, t-1-d_1; ▽, 2-d_1; ○, 3-d_1.

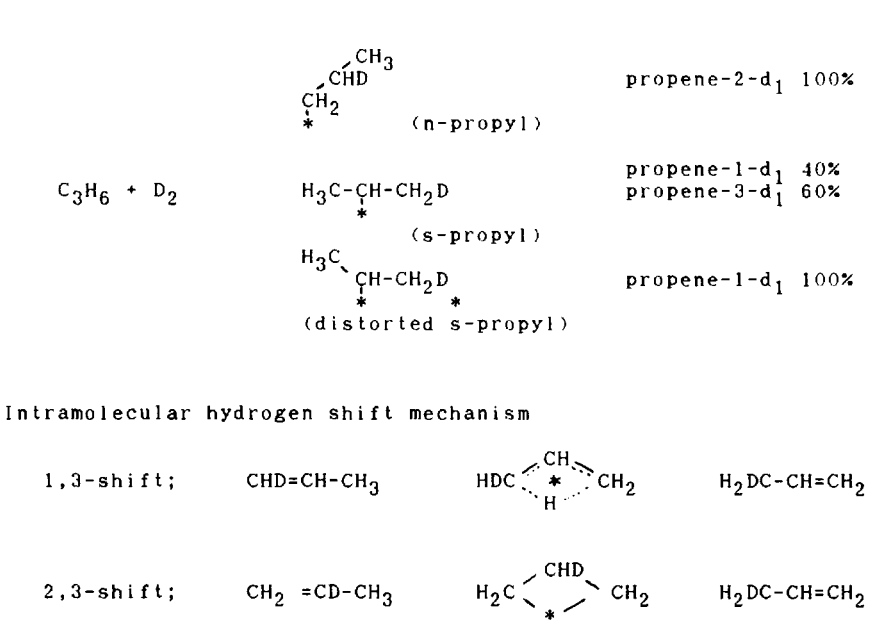

SCHEME 1. Reaction intermediates in hydrogen exchange processes.

the exchange process proceeds through the σ-alkyl intermediates alone, the propene-2-d_1 is formed from *n*-propyl species and propene-1-d_1 and 3-d_1 are formed from *s*-propyl species. The ratio of 1-d_1 and 3-d_1 should be 2 : 3, as summarized in Scheme 1. The experimental ratio (about 30 : 1) obtained from Fig. 3, however, is drastically different from the above expectation and suggests that the two methyl groups of adsorbed *s*-propyl species are not equivalent for the abstraction of a hydrogen atom. Accordingly, we have to suppose some distorted form for adsorbed *s*-propyl species, as shown in Scheme 1.

In addition, if an associative mechanism alone is operating in this C_3H_6–D_2 reaction, the isotope distribution pattern of monodeuteropropene should stay constant at the initial stage of the reaction, where isotopic dilution of deuterium by the repetition of the associative mechanism is not significant. The drastic temporal change in the isotopic distribution shown in Fig. 3 indicates an intramolecular 1,3-hydrogen shift independent of the deuterium incorporation process through the associative mechanism. This was confirmed by the $HDC{=}CH{-}CH_3 + H_2$ reaction, where deuterium exchange by the repetition of σ-alkyl intermediates can be neglected and only the intramolecular hydrogen exchange process can be followed because of the isotopic ratio of H and D (30 : 1) present in the system. The obtained distribution pattern was similar to Fig. 3, which clearly indicated the existence of an intramolecular hydrogen exchange process.

On the other hand, intermolecular hydrogen exchange reactions in the C_3H_6–C_3D_6 system (1 : 1, 12.5 Torr each) proceeded over both unsupported and silica-supported ZrO_2 catalysts at around 473 K. The rate was one order of magnitude slower than the intramolecular 1,3-hydrogen shift process in the C_3H_6–D_2 reaction. The temperature dependence of this process is also displayed in Fig. 2. Note that both catalysts have the same activation energy, 75–76 kcal/mol, for this intermolecular hydrogen exchange process. The isotopic distribution patterns were almost identical on both catalysts: 60% of propene-3-d_1 and 40% of 1-d_1 (same amount of *cis* and *trans* isomers). These results may be explained by assuming that the exchange process proceeds through carbenium ion intermediates (26).

The dependence of the initial rates, as well as of the isotopic distribution pattern of monodeuteropropene in C_3H_6–D_2 reactions, on the amount of ZrO_2 loaded on silica was investigated in the lower loading regions (1–16 wt%). As shown in Fig. 4, the specific rates of propane formation are independent of the amount of ZrO_2 loaded on silica.

3. C_3H_6–D_2 and C_3H_6–C_3D_6 Reactions over ZrO_2/Al_2O_3 and Al_2O_3

The temperature dependence of the C_3H_6–D_2 and C_3H_6–C_3D_6 reactions over alumina-supported catalysts is summarized in Fig. 5, where the reaction rates were normalized as in Fig. 2. Al_2O_3 itself exhibited some activity in these reactions, as seen in the figure. It is characteristic of alumina that hydrogen exchange in the C_3H_6–C_3D_6 reaction (E_a = 33 kJ/mol) is more than one order of magnitude faster than in the C_3H_6–D_2 reaction (E_a = 55 kJ/mol), which is completely opposite to the case of ZrO_2/SiO_2

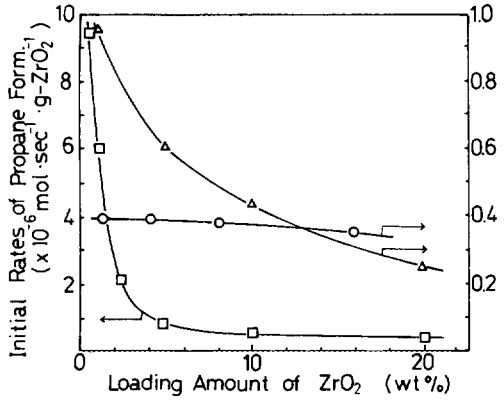

FIG. 4. Dependence of the initial rates of propane formation in C_3H_6–D_2 reactions on the amount of ZrO_2 loaded on various supports. P_{C3H6} = Torr, P_{D2} = 100 Torr. One gram of catalyst. ○, on silica support at 423 K; △, on alumina support at 403 K; □, on titanium dioxide support at 473 K.

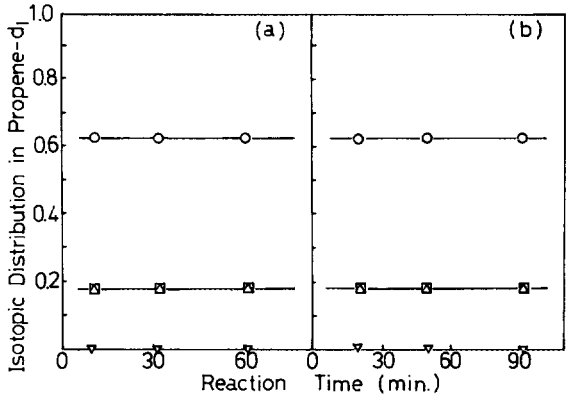

FIG. 6. Time courses of the isotopic distribution in propene-d_1 formed during C_3H_6–C_3D_6 reactions over (a) 1 wt% ZrO_2/Al_2O_3 at 333 K and (b) Al_2O_3 at 383 K. P_{C3H6} = P_{C3D6} = 12.5 Torr. One gram of catalyst. □, c-1-d_1; △, t-1-d_1; ▽, 2-d_1; ○, 3-d_1.

catalysts. When ZrO_2 was dispersed on alumina, the reaction rate in the C_3H_6–D_2 reaction considerably increased with the decrease of the activation energy (E_a = 38 kJ/mol), whereas in the C_3H_6–C_3D_6 reaction the activation energy was almost the same (E_a = 35 kJ/mol). The tendency in the reaction rates was the same as on alumina itself; that is, the C_3H_6–C_3D_6 reaction proceeded much faster than the C_3H_6–D_2 reaction.

Figures 6 and 7 demonstrate the time courses of the overall composition of monodeuteropropenes formed during the C_3H_6–C_3D_6 and C_3H_6–D_2 reactions over ZrO_2/Al_2O_3 and alumina. In the C_3H_6–C_3D_6 reaction, propene-1-d_1 and 3-d_1 were formed in a 2 : 3 ratio on both catalysts. This result indicated the presence of carbenium ion intermediates (26). The isotopic distribution patterns of monodeuteropropene in the C_3H_6–D_2 reaction over 1 wt% ZrO_2/Al_2O_3 and alumina itself are similar to those in the C_3H_6–C_3D_6 reaction, that is, a 2 : 3 ratio of propene-1-d_1 and 3-d_1 with a small amount of propene-2-d_1. Considerably different activation energies in these two reactions on alumina suggest that dissociation of deuterium molecules may be the rate-determining step in the C_3H_6–D_2 reaction, and that once deuterium is incorporated into propene via an associative mechanism, intermolecular hydrogen exchange of propene proceeds rapidly through carbenium ion intermediates.

The dependence on the amount of ZrO_2 loaded on alumina of the initial rates of propane formation in C_3H_6–D_2 reactions was investigated and shown in Fig. 4.

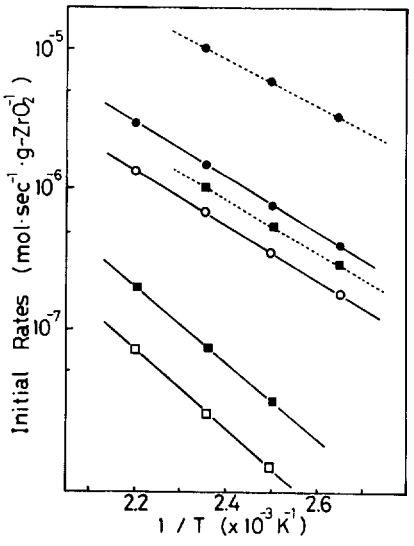

FIG. 5. Temperature dependence of C_3H_6–D_2 reactions (solid lines; P_{C3H6} = 25 Torr, P_{D2} = 100 Torr) and C_3H_6–C_3D_6 reactions (broken lines; P_{C3H6} = P_{C3D6} = 12.5 Torr) over ZrO_2/Al_2O_3 and Al_2O_3. One gram of catalyst. Open and closed symbols refer to the initial rates of propane and propene-d_1 formations, respectively. ○●, 1 wt% ZrO_2/Al_2O_3; □■, Al_2O_3.

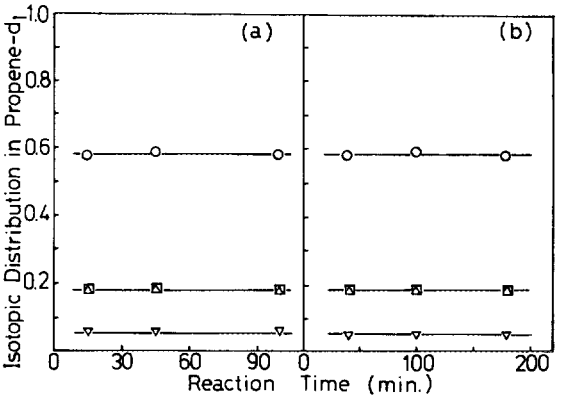

FIG. 7. Time courses of the isotopic distribution in propene-d_1 formed during C_3H_6–D_2 reactions over (a) 1 wt% ZrO_2/Al_2O_3 at 373 K and (b) Al_2O_3 at 423 K. P_{C3H6} = 25 Torr. P_{D2} = 100 Torr. One gram of catalyst. □, c-1-d_1; △, t-1-d_1; ▽, 2-d_1; ○, 3-d_1.

4. C_3H_6–D_2 and C_3H_6–C_3D_6 Reactions over ZrO_2/TiO_2 and TiO_2

The temperature dependences of the C_3H_6–D_2 and C_3H_6–C_3D_6 reaction rates over ZrO_2/TiO_2 and TiO_2 are summarized in Fig. 8. In the case of the C_3H_6–D_2 reaction over TiO_2, the activation energy of the propene-d_1 formation by the exchange process (71 kJ/mol) was much larger than that of propane formation by the addition process (52 kJ/mol) and similar to that of the C_3H_6–C_3D_6 reaction (75 kJ/mol). Figure 9 shows the result of the microwave spectroscopic analysis of propene-d_1 and demonstrates the identical deuterium distribution pattern in both reactions. Thus hydrogen exchange in the C_3H_6–D_2 reaction proceeds through a different intermediate than that for the process of deuterium addition to form propane and through the same intermediate as that in the C_3H_6–C_3D_6 reaction. This result is same as that over unsupported ZrO_2 itself, mentioned in section 2.

Over ZrO_2 dispersed on TiO_2, the rate of the C_3H_6–D_2 reaction considerably increased with the decrease of the activation energy (for propane formation, from 52 kJ/mol on TiO_2 to 36 kJ/mol on ZrO_2/TiO_2). The hydrogen exchange process then exhibited the same activation energy (36 kJ/mol) as the addition process, which indicated that both processes proceeded through the same adsorbed propyl intermediates via associative mechanisms. The reaction rate greatly depended on the loading amount of ZrO_2, and 1 wt% catalysts exhibited much higher activity than 10 wt% catalysts, although their activation energy

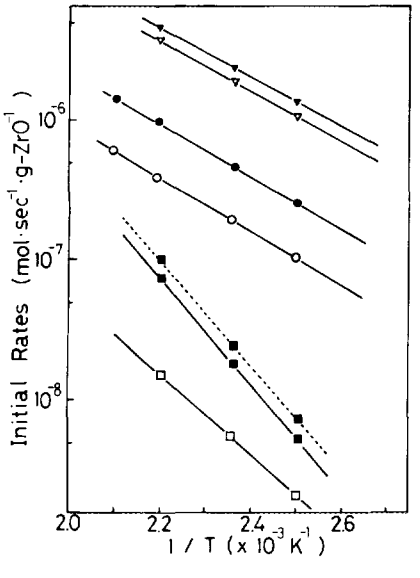

FIG. 8. Temperature dependence of C_3H_6–D_2 reactions (solid lines; P_{C3H6} = 25 Torr, P_{D2} = 100 Torr) and C_3H_6–C_3D_6 reactions (broken lines; P_{C3H6} = P_{C3D6} = 12.5 Torr) over ZrO_2/TiO_2 and TiO_2. One gram of catalyst. Open and closed symbols refer to the initial rates of propane and propene-d_1 formation, respectively. ▽▼, 1 wt% ZrO_2/TiO_2; ○●, 10 wt% ZrO_2/TiO_2; □■, TiO_2.

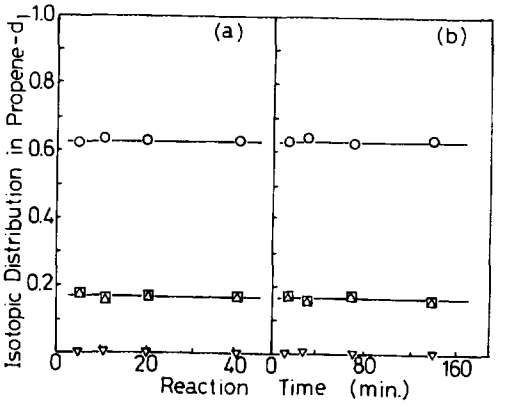

FIG. 9. Time courses of the isotopic distribution in propene-d_1 formed during (a) C_3H_6–D_2 (P_{C3H6} = 25 Torr, P_{D2} = 100 Torr) and (b) C_3H_6–C_3D_6 (P_{C3H6} = P_{C3D6} = 12.5 Torr) reactions over TiO_2 catalyst. One gram of catalyst. □, c-1-d_1; △, t-1-d_1; ▽, 2-d_1; ○, 3-d_1.

was almost the same. The dependence of the initial rates of propane formation in C_3H_6–D_2 reaction upon the amount of ZrO_2 loaded on TiO_2 was summarized in Fig. 4.

Figure 10 demonstrates the isotopic distribution pattern of monodeuteropropene during the C_3H_6–D_2 reaction over 1 and 10 wt% ZrO_2/TiO_2. At the initial stage of the exchange process over 1 wt% catalyst, propene-2-d_1 was the main product through *n*-propyl intermediates. The subsequent rapid decrease in 2-d_1 species was accompanied by an increase in propene-3-d_1. This finding may be explained by an independent intramolecular 2,3-hydrogen shift in propene following the incorporation of deuterium through *n*-propyl species. To confirm this, the propene-2-d_1 + H_2 reaction was carried out and a distribution pattern similar to that in Fig. 10(a) clearly indicated the presence of intramolecular hydrogen shift processes. In the case of 10 wt% ZrO_2/TiO_2, the pattern was completely different than that for 1 wt% catalyst, as shown in Fig.

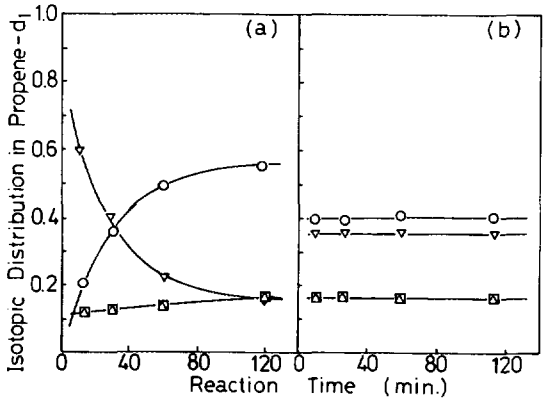

FIG. 10. Time courses of the isotopic distribution in propene-d_1 formed during C_3H_6–D_2 reactions over (a) 1 wt% and (b) 10 wt% ZrO_2/TiO_2. P_{C3H6} = 25 Torr, P_{D2} = 100 Torr. One gram of catalyst. □, c-1-d_1; △, t-1-d_1; ▽, 2-d_1; ○, 3-d_1.

10(b), and *s*-propyl intermediates were more active than *n*-propyl species for the exchange process.

DISCUSSION

The unique character of metal oxides as hydrogenation catalysts has been reported for ethene over Cr_2O_3 (21), ZnO (22, 23), and Co_3O_4 (22) and for 1,3-butadiene over ZnO (24) and MgO (25). In these reactions, H_2 (or D_2) maintains its molecular identity; that is, both H (or D) atoms in a H_2 (or D_2) molecule are incorporated into a single hydrogenated molecule. Accordingly, in the olefin–D_2 reaction, d_2-paraffin is the main product, as in the case of unsupported ZrO_2. The detailed mechanism of the hydrogenation of ethene over ZnO was examined by Dent and Kokes (27, 28) by kinetic investigation as well as infrared spectroscopy. To interpret the molecular identity of the added hydrogen atoms, it was postulated that an isolated Zn–O ion pair, surrounded by lattice O^{2-}, was the active site.

Since the catalytic behavior of unsupported ZrO_2 is very similar to that of ZnO, it would be reasonable to suppose that isolated Zr–O ion pairs are active sites for propene hydrogenation in the present study. The question now is how this surface structure is transformed by supporting ZrO_2 on silica. To clarify this point, we attempted to vary the dispersion of ZrO_2 on silica by changing the amount of loading and to examine its influence upon the reaction rates as well as the reaction mechanisms. As shown in Fig. 4, the initial specific rates of deuterium addition in the C_3H_6–D_2 reaction were independent of the amount of ZrO_2 loaded on silica in the lower loading regions (1–16 wt%). This is consistent with the results of XPS analysis that estimated coverages (θ_{XPS}) of ZrO_2 are proportional to the amount of loading, which indicates the formation of monolayers of zirconia over silica supports. Accordingly, on the surfaces of such a two-dimensional network of ZrO_2, there are no isolated Zr–O ion pairs surrounded by O^{2-} ions that block the reverse process from Zr-propoyl species to propene. Thus on the silica-supported ZrO_2 catalyst hydrogen exchange of propene becomes accessible as well as the addition process to form propane.

The situation was different in the cases of alumina-supported catalysts. In the C_3H_6–C_3D_6 reaction, although the exchange rate was increased more than one order of magnitude, the activation energies were almost the same over ZrO_2/Al_2O_3 and alumina. Microwave spectroscopic analysis revealed that carbenium ions may be reaction intermediates over both catalysts. Accordingly, it is reasonable to suppose that the amount of acidic sites was considerably increased by dispersing ZrO_2 on the alumina surface.

On the other hand, hydrogen exchange in the C_3H_6–D_2 reaction on alumina was much slower and had higher activation energy than in the C_3H_6–C_3D_6 reaction on alumina. However, the isotopic distribution pattern was almost the same as that of the C_3H_6–C_3D_6 reaction, with a small amount of propene-2-d_1. As discussed under results these phenomena may be explained by assuming that the dissociation of deuterium is the rate-determining step in C_3H_6–D_2 reactions, and deuterium incorporated in propene by associative mechanisms is redistributed by carbenium ion intermediates to give a 2 : 3 ratio of propene-1-d_1 and 3-d_1.

Dispersing ZrO_2 on alumina caused a considerable increase of the C_3H_6–D_2 reaction rate with the decrease of activation energy. However, the catalytic behavior (as shown, for example, by the isotopic distribution pattern of monodeuteropropene) was almost the same as on alumina itself. These results suggest that over ZrO_2/Al_2O_3, deuterium molecules will dissociate on the ZrO_2 surface, spill over toward the alumina surface, and react with adsorbed propene to form propyl intermediates. The redistribution of deuterium atoms in the 1- and 3-positions of propene proceeds independently through a carbenium ion intermediate. To confirm this, the C_3H_6–C_3D_6–D_2 reaction was carried out on ZrO_2/Al_2O_3. The same isotopic distribution pattern as in Fig. 6(a) was observed, but with a slower formation of propane. The dependence of the initial rate of propane formation on the amount of ZrO_2 loading on alumina is summarized in Fig. 4. The gradual decrease of the specific rate per gram of ZrO_2 may correspond to the decrease in dispersion with decreased loading amount as shown by XPS analysis (Table 1).

In the case of TiO_2 catalyst, the hydrogen exchange process via hydrogen abstraction from adsorbed propyl species seems to be very slow in the C_3H_6–D_2 reaction and an independent hydrogen exchange process exists in the C_3H_6–C_3D_6 reaction. When 0.5–1.0 wt% ZrO_2 was dispersed on the TiO_2 surface, the characteristic features of TiO_2 itself disappeared completely, and both deuterium addition and exchange began to take place through the same n-propyl adsorbed species. These results indicate that the number of active sites on TiO_2 for propene hydrogenation is rather small and that ZrO_2 may be dispersed selectively to create some specific sites that are active for these reactions. As shown in Fig. 4, an increase in the loading amount of ZrO_2 drastically decreased the specific rate and *s*-propyl adsorbed species became the main active intermediate.

CONCLUSIONS

Quantitative XPS analysis revealed the formation of a ZrO_2 monolayer over the silica surface of up to 10 wt% ZrO_2/SiO_2 catalysts. Although a monolayer of ZrO_2 may be formed over alumina and titania surfaces in the cases

of 1 wt% ZrO_2/Al_2O_3 and ZrO_2/TiO_2 catalysts, crystals of ZrO_2 seems to grow when more ZrO_2 are loaded. Dispersed ZrO_2 over these supports exhibited much high activity and lower activation energy than unsupported ZrO_2 for propene–deuterium addition and exchange reactions. Over ZrO_2/SiO_2 catalysts, a two-dimensional network of ZrO_2 makes the reverse process of propyl intermediate formation accessible. In the case of ZrO_2/Al_2O_3 catalysts, deuterium dissociation takes place preferentially over a dispersed ZrO_2 surface, spills over toward the alumina support, and reacts with adsorbed propene on alumina. The marked enhancement of the reaction rate over 1 wt% ZrO_2/TiO_2 catalysts can be explained by the strong interaction of zirconium monolayers with the active sites of TiO_2 surfaces.

REFERENCES

1. Boudart, M., *Adv. Catal.* **20,** 153 (1969).
2. Boudart, M., J. *Mol. Catal.* **30,** 27 (1985).
3. Somorjai, G. A., and Carrazza, J., *Ind. Eng. Chem. Fundam.* **25,** 63 (1986).
4. Hardcastle, F. D., Wachs, I. E., Horsley, J., and Via, G. H., *J. Mol. Catal.* **46,** 15 (1988).
5. Kozlowski, R., *Bull. Pol. Acad. Sci. Chem.* **35,** 365 (1986).
6. Kozlowski, R., Pettifer, R. F., and Thomas, J. M., *J. Phys. Chem.* **87,** 5176 (1983).
7. Kobayashi, H., Yamaguchi, M., Tanaka, T., Nishimura, Y., Kawakami, H., and Yoshida, S., *J. Phys. Chem.* **92,** 2516 (1988).
8. Chieu, N. S., Bauer, S. H., and Johnson, M. F. L., *J. Catal.* **89,** 226 (1984).
9. Horsley, J. A., Wachs, I. E., Brown, J. M., Via, G. H., and Hardcastle, F. D., *J. Phys. Chem.*, **91,** 4014 (1987).
10. Deo, G., and Wachs, I. E., *J. Phys. Chem.* **95,** 5889 (1991).
11. Hattori, T., Matsuda, M., Suzuki, K., Miyamoto, A., and Murakami, Y., "Proceedings, 9th International Congress on Catalysis, Calgary, 1988" (M. J. Phillips and M. Ternan, Eds.), p. 1640. Chem. Institute of Canada, Ottawa, 1988.
12. Okamoto, Y., Tomiok, H., Katoh, Y., Imanaka, T., and Teranishi, S., *J. Phys. Chem.* **84,** 1833 (1980).
13. Naito, S., Tanimoto, M., Soma, M., and Udagawa, Y., *Stud. Surf. Sci. Catal.* **75,** 2043 (1993).
14. Naito, S., and Tanimoto, M., *J. Catal.* **102,** 337 (1986).
15. Norris, W. P., *J. Org. Chem.* **24,** 1579 (1959).
16. Angevine, P. J., Delgass, W. N., and Vartuli, J. C., "Proceedings, 6th International Congress on Catalysis, London, 1976" (G. C. Bond, P. B. Wells, and F. C. Tompkins, Eds.) The Chemical Society, London, 1977.
17. Kerkhof, F. P. J. M., and Moulijin, J. A., *J. Phys. Chem.* **83,** 1612 (1979).
18. Davis, S. M., *J. Catal.* **117,** 432 (1989).
19. Seyama, H., and Soma, M., *Res. Rep. Nat. Inst. Environ. Stud. Jpn.* **38,** 23 (1982).
20 Yamaguchi, T., and Hightower, J. W., *J. Am. Chem. Soc.* **99,** 4201 (1977).
21 Carwell, M., and Burwell, R. L., Jr., *J. Am. Chem. Soc.* **82,** 6289 (1960).
22. Conner, W. C., Innes, R. A., and Kokes, R. J., *J. Am. Chem. Soc.* **90,** 6858 (1968).
23. Conner, W. C., and Kokes, R. J.,. *J. Phys. Chem.* **73,** 2436 (1969).
24. Naito, S., Sakurai, Y., Shimizu, H., Onishi, T., and Tamaru, K., *Bull. Chem. Soc. Jpn.* **43,** 2274 (1970); *Trans. Faraday Soc.* **67,** 1529 (1971).
25. Hattori, Y., Tanaka, Y., and Tanabe, K., *J. Am. Chem. Soc.* **98,** 4652 (1976).
26. Kondo, T., Saito, S., and K. Tamaru, *J. Am. Chem. Soc.* **96,** 6857 (1974).
27. Dent, A. L., and Kokes, R. J. *J. Am. Chem. Soc.* **91,** 7207 (1969).
28. Dent, A. L., and Kokes, R. J., *J. Phys. Chem.* **73,** 3772, 3781 (1969).